Polymer 49 (2008) 3693–3701

Contents lists available at ScienceDirect

Polymer

journal homepage: www.elsevier.com/locate/polymer

Tacticity control by conformational isomerization in free radical polymerization of acrylate

Hitoshi Tanaka*, Miki Niwa

Institute of Technology and Science, University of Tokushima, Minamijosanjima-cho, Tokushima 770-8506, Japan

ARTICLE INFO

Article history:
Received 19 February 2008
Received in revised form 24 June 2008
Accepted 26 June 2008
Available online 2 July 2008

Keywords:
Radical polymerization
Tacticity
Acrylate

ABSTRACT

Contribution of conformational isomerization to polymer tacticity has been studied in free radical polymerization of (−)-menthyl 2-acetamidoacrylate with azo initiators. It has been demonstrated that the chain end of the growing polymer radical, which is generated from the s-*trans* and s-*cis* conformers of monomer, produces stereoselectively new *R* and *S* configurational quaternary carbons, respectively, for the attack of monomer. In addition, polymerization reactivity of both conformers is indistinguishable under the present conditions, and the polymerization is considered to proceed through a chain-end controlled mechanism, which excludes a penultimate unit effect on tacticity in the polymerization. The results obtained would give a clue to understand an origin of tacticity in conventional free radical polymerization of acrylates.

1. Introduction

The majority of research in radical polymerization has focused on the stereoregulation of polymer and polymerization [1,2]. Control of tacticity, in particular, has extensively been interested and the polymerization of olefins bearing bulky substituents or the polymerization in the presence of coordination reagents, polymer matrices, and inclusion compounds has been studied to obtain a high isotactic or syndiotactic polymer [3]. Lewis acids [4,5] and solvents like alcohols [6], for instance, form a complex with radical and/or monomer to change the bulkiness and spin density [7] of the substrates and sometimes enhance the isotacticity of the resulting polymer, e.g., isotacticity from 7 to 63% for the polymerization of *N*-methyl methacrylamide by the addition of $Yb(OTf)_3$ [8]. In replica polymerization of methyl methacrylate, syndiospecific [9] and isospecific [10] propagations have taken place in the presence of the isotactic and syndiotactic polymer matrices, respectively. High isotacticity of polymer has also been performed using bulky olefins substituted by aryl group in the ester moiety, e.g., achiral arylmethyl methacrylates [11], *N*-arylmethyl methacrylamides [12], and diphenyl acrylamides [13]. The origin of these stereospecific radical polymerizations, however, has little been revealed yet, and the mechanism of the polymerizations has only abstractly been concluded to some steric hindrance or a complexation between substrates without any further precise argument.

Several groups have been employed chiral auxiliary to control the stereochemistry in radical additions of small molecules including α,β-unsaturated amides [14–16], Oppolzer's camphor sultam [17], fumarates [18], and they have discussed on the mechanism of the stereospecificity. Porter and his coworkers have studied the control of the stereochemistry of radical additions, e.g., dimerization and trimerization, of chiral acrylamide, and found that pyrrolidine acrylamide would give two stereoisomers with *S* and *R* configurations for the attack of α-amide radical in large excess of one isomer to the other [14,15]. High selectivity similar to the pyrrolidine has also been observed in the radical reactions of chiral oxazolidine acrylamide [16]. Interestingly, the oxazolidine can polymerize to give a polymer with isotacticity as high as 92% [16]. The mechanism giving preferentially isotactic sequence is believed to be the result of one-sided facial selectivity in the addition of the monomer to the same growing radical face caused by the chiral auxiliary. Presence of chiral center in acrylamide derivatives, however, does not always lead to an isotactic polymer. Radical polymerization of chiral acrylamidosulfonic acids, for instance, has been known to give essentially an atactic polymer [19]. As is well known, an amide has a rigid structure, i.e., the rotation around carbon–nitrogen bond is restricted by the conjugation of π electron of C═O group with a lone pair on nitrogen atom [15]. Thus, most of the stereospecific chiral auxiliary radical polymerizations have concerned to an amide monomer. Unfortunately, however, the mechanism giving such an isotactic or atactic polymer has not been revealed yet even for an amide polymerization.

We report herein how tacticity can arise in free radical polymerization of acrylates, e.g., why the probability of *meso*- or *racemo*-propagation, P_m or P_r, cannot become 0.5 in most of the

* Corresponding author.
E-mail address: tanaka@opt.tokushima-u.ac.jp (H. Tanaka).

0032-3861/$ – see front matter © 2008 Elsevier Ltd. All rights reserved.
doi:10.1016/j.polymer.2008.06.042

radical polymerizations, e.g., P_m typically lies in the range 0.4–0.5 for vinyl monomers and 0.2–0.5 for 1,1-disubstituted monomers [20]. It has been reported for acrylate (**1**) used in this study that an isotacticity of polymer increases with increasing conversion (tacticity mutating polymerization), i.e., decreasing monomer concentration even in conventional conditions at moderate temperature, and in the polymerization near ceiling temperature **1** generates a helical polymer (Scheme 1) [21]. However, **1** can give a random coil atactic polymer at the polymerization temperature far from a ceiling temperature (T_c), e.g., 30 °C ($T_c = 75.4$ °C in [**1**] = 2.0 mol/l in benzene) [22]. Well-known chiral auxiliary radical polymerization of amides and indene [23] is an isospecific polymerization system, and therefore it may be distinguished from a conventional radical polymerization system.

2. Experimental

2.1. Materials

Compound **1** was prepared according to the previous procedure [22], and purified by a column chromatography using a mixture of *n*-hexane and ethylacetate (4:1 wt-ratio) as a developing solvent, $[\alpha]_D = -81.0°$ in $CHCl_3$. ^1H NMR ($CDCl_3$, TMS, ppm) for **1**: 0.76 (d, $J = 7.1$ Hz, 3H, CH_3), 0.90 (d, $J = 7.1$ Hz, 3H, CH_3), 0.92 (d, $J = 6.6$ Hz, 3H, CH_3), 1.0–2.0 (m, 9H, menthyl), 2.13 (s, 3H, $COCH_3$), 4.80 (dt, $J = 4.5$, 11 Hz, 1H, menthyl), 5.85 (s, 1H, CH═), 6.57 (s, 1H, CH═), 7.94 (br s, 1H, NH). Anal. Calcd for $C_{15}H_{25}NO_3$: C, 68.04; H, 9.41; N, 4.87. Found: C, 67.90; H, 9.38; N, 5.02. Commercial grade 2,2′-azobis(4-methoxy-2,4-dimethylvaleronitrile) (AMVN), 2,2′-azobis(isobutyronitrile) (AIBN), and 2,2′-azobis(2,4-dimethylvaleronitrile) (ADVN) (Wako Pure Chemicals Co.) were purified by recrystallizations from methanol for AMVN and AIBN and *n*-hexane for ADVN. Deuterated solvent including $CDCl_3$ used for NMR measurement was purchased from Acros Organics Co.

2.2. Measurements

^1H NMR spectrum was recorded on JEOL EX-400 (400 MHz) spectrometer in $CDCl_3$ at 25 °C using tetramethylsilane as an internal standard. ^{13}C NMR spectrum at 100 MHz was measured in 3 wt% D_2O solution at 80 °C with dimethylsulfoxide as an internal standard using JEOL EX-400 spectrometer under conditions of full proton decoupling in 5 mm tube. Typical conditions in ^{13}C NMR spectrum measurements were as follows: sweep width: 20,000 Hz, data point: 32,000, pulse angle: 90°, pulse delay: 2.46 s, and accumulation: 50,000 scans. FT-IR spectrum was recorded in neat or nujol at ambient temperature on JASCO FT/IR-8900 spectrometer. Specific rotation $[\alpha]_D$ at $\lambda = 589.3$ nm (Na–D) was measured on JASCO DIP-360 digital polarimeter in $CHCl_3$ at ambient temperature. Circular dichroism (CD) was recorded on JASCO J-820 spectropolarimeter in ultra-pure *n*-hexane (Wako Pure Chemicals Co.) at 20 °C. Number-average molecular weight (M_n) of polymer was determined by size exclusion chromatography (SEC) using a Tosoh HLC 8020 (Column: TSKgel G7000HHR + G5000HHR + G3000) in tetrahydrofuran at 35 °C on the basis of standard polystyrene. X-Ray diffraction was measured with Rigaku RAXIS-Rapid imaging plate diffractometer using graphic monochromated Cu Kα radiation ($\lambda = 1.54178$ Å) at 23 °C to a maximum 2θ value of 136.1°.

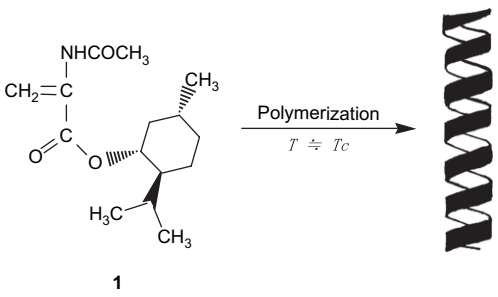

1

Scheme 1. Formation of helical structure in radical polymerization of **1** near ceiling temperature.

2.3. Polymerization

Polymerization was carried out in benzene in a sealed pyrex glass ampoule with shaking at given temperature. The ampoule which contains required amounts of reagents including initiator, solvent, and monomer (2.0 mol/l) was degassed several times by a freeze–thaw method and then sealed under reduced pressure and placed in a constant temperature bath. After the polymerization, the resulting polymer was isolated by pouring the contents of the ampoule into a large amount of methanol. For a photopolymerization, it was performed with ADVN in benzene solution using high pressure mercury lamp (300 W) as a light source in a constant temperature bath at given temperature. The polymers used for the measurements of specific rotation, and CD, NMR, and IR spectra, and SEC were further purified by reprecipitations from the benzene solution into methanol. Finally, the polymer was dried under vacuum at ambient temperature for several days and identified.

2.4. Hydrolysis

Polymer was hydrolyzed with KOH. A solution of KOH (1.0 g) in methanol (30 ml) was added dropwise to benzene solution (20 ml) of polymer (0.2 g) for 1 h at ambient temperature. The precipitated polymer was filtered on a grass filter, and it was further refluxed in KOH (1.0 g) aqueous solution (10 ml) for 2 days. The resultant solution after partial (5.0 ml) removal of water with an evaporator was poured into a large amount of methanol to isolate a hydrolyzed polymer. The reaction proceeded quantitatively, and the polymer furnished for NMR measurement was purified by reprecipitations from the aqueous solution into methanol followed by vacuum drying.

2.5. Hydrogenation

Hydrogenation of **1** was carried out with Pd/C for 48 h under H_2 atmosphere in dry CH_2Cl_2 at ambient temperature. The reaction gave quantitatively a mixture of two isomers of (*R*)-**1a** and (*S*)-**1a**, which were isolated by recrystallization from *n*-hexane, $[\alpha]_D = -72.0°$ for (*R*)-**1a** and $[\alpha]_D = -56.4°$ for (*S*)-**1a** in $CHCl_3$ at ambient temperature. ^1H NMR ($CDCl_3$, TMS, ppm) for (*R*)-**1a**: δ 0.745 (d, $J = 6.8$ Hz, 3H, CH_3), 0.86–0.92 (m, 6H, CH_3), 0.90–1.9 (m, 9H, menthyl), 1.394 (d, $J = 6.8$ Hz, 3H, CH_3), 2.01 (s, 3H, $COCH_3$), 4.70 (dt, $J = 4.2$, 11 Hz, 1H, menthyl), 6.19 (br d, $J = 6.1$ Hz, 1H, NH). IR (nujol, cm^{-1}) for (*R*)-**1a**: 3343 (ν_{NH}), 1720 ($\nu_{C=O}$, ester), 1685 ($\nu_{C=O}$, amide). ^1H NMR ($CDCl_3$, TMS, ppm) for (*S*)-**1a**: δ 0.754 (d, $J = 6.6$ Hz, 3H, CH_3), 0.86–0.92 (m, 6H, CH_3), 0.90–1.9 (m, 9H, menthyl), 1.387 (d, $J = 6.4$ Hz, 3H, CH_3), 2.01 (s, 3H, $COCH_3$), 4.73 (dt, $J = 4.3$, 11 Hz, 1H, menthyl), 6.19 (br d, $J = 6.1$ Hz, 1H, NH). IR (nujol, cm^{-1}) for (*S*)-**1a**: 3343 (ν_{NH}), 1721 ($\nu_{C=O}$, ester), 1652 ($\nu_{C=O}$, amide). Crystals of (*R*)-**1a** and (*S*)-**1a** were produced by relatively first and slow recrystallizations from *n*-hexane, respectively, and stereochemistry was assigned by X-ray crystallography.

2.6. Tin hydride reaction

A toluene solution of (n-C_4H_9)$_3$SnH (0.8 mM), AIBN (0.8 mM), benzylbromide (8 mM), and **1** (0.8 mM) was heated at 80 °C for 12 h, and then AIBN (0.8 mM) and benzylbromide (8 mM) were further added to the reaction mixture and they were subsequently heated at 80 °C for 12 h. After reaction, products were passed through silica gel (Kanto Chemical Co., 60 N) in a mixed solvent of n-hexane and ethylacetate (4:1 wt-ratio) to isolate addition product (*R*)-**1b**. After removing (*R*)-**1b**, eluents free from by-products were collected and again passed through Shiseido C18 column (acetonitrile:H_2O = 5:2 wt-ratio) to get (*S*)-**1b**. The by-products which contain small fragments and oligomers have not yet been characterized. Isolated (*R*)-**1b** and (*S*)-**1b** were further purified by recrystallization from n-hexane and they were used for X-ray diffraction measurements. Total yield of (*R*)-**1b** and (*S*)-**1b** was 10%, and the molar ratio of (*R*)-**1b**/(*S*)-**1b** in the reaction mixture was determined by high pressure liquid chromatography (JASCO 880-PU) with UV–vis detector using Shiseido C18 column in a mixed solvent of acetonitrile and H_2O (3:1 wt-ratio). $[\alpha]_D = -93.3°$ for (*R*)-**1b** and $[\alpha]_D = -4.0°$ for (*S*)-**1b** in $CHCl_3$ at ambient temperature. ^{1}H NMR ($CDCl_3$, TMS, ppm) for (*R*)-**1b**: δ 0.77 (d, J = 7.1 Hz, 3H, CH_3), 0.91 (m, 6H, CH_3), 0.90–2.25 (m, 9H, menthyl), 2.53–2.72 (m, 2H, CH_2), 1.61 (s, 2H, CH_2), 1.99 (s, 3H, $COCH_3$), 4.65–4.69 (m, 1H, H), 4.74 (dt, J = 4.4, 10.9 Hz, 1H, menthyl), 6.03 (br d, J = 7.8 Hz, 1H, NH), 7.14–7.30 (m, 5H, benzyl). IR (nujol, cm^{-1}) for (*R*)-**1b**: 3266 (ν_{NH}), 1733 ($\nu_{C=O}$, ester), 1645 ($\nu_{C=O}$, amide). ^{1}H NMR ($CDCl_3$, TMS, ppm) for (*S*)-**1b**: δ 0.76 (d, J = 6.9 Hz, 3H, CH_3), 0.89 (m, 6H, CH_3), 0.90–2.23 (m, 9H, menthyl), 2.54–2.71 (m, 2H, CH_2), 1.58 (s, 2H, CH_2), 1.99 (s, 3H, $COCH_3$), 4.64–4.69 (m, 1H, H), 4.76 (dt, J = 4.4, 10.9 Hz, 1H, menthyl), 6.03 (br d, J = 7.6 Hz, 1H, NH), 7.15–7.31 (m, 5H, benzyl). IR (nujol, cm^{-1}) for (*S*)-**1b**: 3243 (ν_{NH}), 1742 ($\nu_{C=O}$, ester), 1639 ($\nu_{C=O}$, amide).

2.7. X-ray analysis

All diffraction measurements were carried out on a Rigaku RAXIS-RAPID imaging Plate diffractometer with graphite-monochromated Cu Kα (λ = 1.54178 Å) radiation. Data were collected at 23.0°. The structure was solved by direct methods using SIR92 [24] for (*R*)-**1a** and SHELX-97 [25] for (*S*)-**1a**, (*R*)-**1b**, and (*S*)-**1b**. The non-hydrogen atoms were refined anisotropically. Hydrogen atoms were included but not refined. Crystal data of (*R*)-**1a**: formula $C_{15}H_{27}NO_3$; weight 269.38; crystal system trigonal; space group $P3_221$; a 8.0479(2), c 44.290(2) Å; V 2484.3(1) Å^3; Z 4; D_{calcd} 1.080 g cm^3; F(000) 888.00; μ 5.93 cm^{-1}; crystal size 0.35 × 0.06 × 0.35 mm; $2\theta_{max}$ 136.1°; reflections collected 27,564; unique 3023 (R_{int} = 0.041); parameter 172; R 0.045; Rw 0.105; GOF 1.02. (*S*)-**1a**: formula $C_{15}H_{27}NO_3$; weight 269.38; crystal system monoclinic; space group $P2_1$; a 5.0085(3), b 11.2251(7), c 14.549(1) Å; β 98.205(3)°; V 809.58(9) Å^3; Z 2; D_{calcd} 1.105 g cm^3; F(000) 296.00; μ 6.07 cm^{-1}; crystal size 0.45 × 0.40 × 0.05 mm; $2\theta_{max}$ 136.5°; reflections collected 8825; unique 2826 (R_{int} = 0.041); parameter 172; R1 0.041; Rw 0.110; GOF 1.28. (*R*)-**1b**: formula $C_{22}H_{33}NO_3$; weight 359.49; crystal system monoclinic; space group $P2_1$; a 10.5548(8), b 9.1544(5), c 12.3230(10) Å; V 1111.52(14) Å^3; Z 2; D_{calcd} 1.074 g cm^3; F(000) 392.00; μ 5.55 cm^{-1}; crystal size 0.50 × 0.25 × 0.25 mm; $2\theta_{max}$ 134.9°; reflections collected 11,887; unique 2082 (R_{int} = 0.055); parameter 279; R1 0.066 ($I > 2\sigma(I)$); wR2 0.179; GOF 1.04. (*S*)-**1b**: formula $C_{22}H_{33}NO_3$; weight 359.49; crystal system orthorhombic; space group $P2_12_12_1$; a 8.8776(3), b 13.1591(7), c 19.4847(10) Å; V 2276.23(19) Å^3; Z 4; D_{calcd} 1.049 g cm^3; F(000) 784.00; μ 5.42 cm^{-1}; crystal size 0.65 × 0.40 × 0.05 mm; $2\theta_{max}$ 135.9°; reflections collected 22,910; unique 2271 (R_{int} = 0.057); parameter 287; R1 0.056 ($I > 2\sigma$(I)); wR2 0.138; GOF 1.00.

3. Results and discussion

3.1. Hydrogenation

In order to compare the structure of polymer with that of the corresponding monomeric model, **1** was hydrogenated with palladium-activated carbon (Pd/C) catalyst under H_2 atmosphere. The reaction proceeded quantitatively to give two products (Scheme 2) which fortunately formed single crystals suitable for X-ray crystallographic analysis. The analyses were successfully performed and the molecular structures are illustrated in Fig. 1. As seen in this figure, both products, i.e., (*R*)-**1a** and (*S*)-**1a**, are diastereoisomers with each other which have *R* and *S* configurations at newly formed chiral carbon. The ratio of (*R*)-**1a**/(*S*)-**1a** was estimated to be 61.8:38.2 by ^{1}H NMR spectrum of the reaction mixture as shown in Fig. 2. In this figure, a pair of a quartet of doublet due to the menthyl methine proton appears in the region of 4.65–4.77 ppm, where each set of the lower and higher magnetic fields can be assigned to the diastereoisomers with *S* and *R* configurations at newly formed chiral carbon, respectively, in comparison with the spectrum of isolated (*S*)-**1a** and (*R*)-**1a**. It is noted that the *R*/*S* ratio (61.8:38.2) in NMR is comparable to the s-*trans*/s-*cis* rotamer ratio (62.4:37.6) of **1** in IR spectrum (Fig. 3), indicating that the stereochemistry of the hydrogenation is controlled by the conformation of **1**. Very small discrepancies between the *R*/*S* ratio and the s-*trans*/s-*cis* ratio may be explained in terms of difference in molar absorption coefficient of each isomer [26] and errors in measuring in IR spectrum. It is of interest that the result obtained in the hydrogenation demonstrates that the interconversion between s-*trans* and s-*cis* conformers is restricted enough to be distinguished even in an early stage of coordination to Pd/C catalyst since a hydrogenation of olefin with

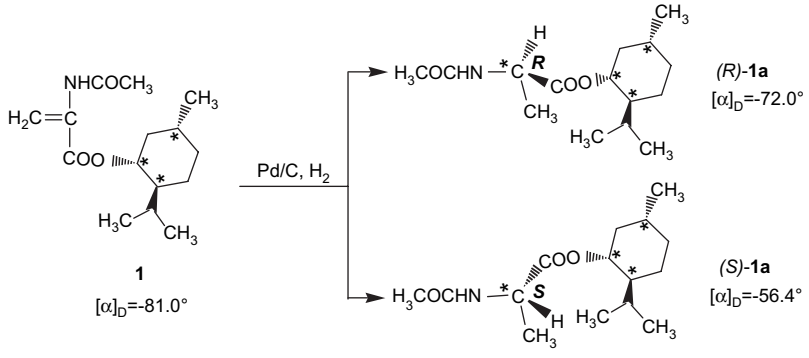

Scheme 2. Reaction products in hydrogenation of **1** using Pd/C catalyst under H_2 atmosphere.

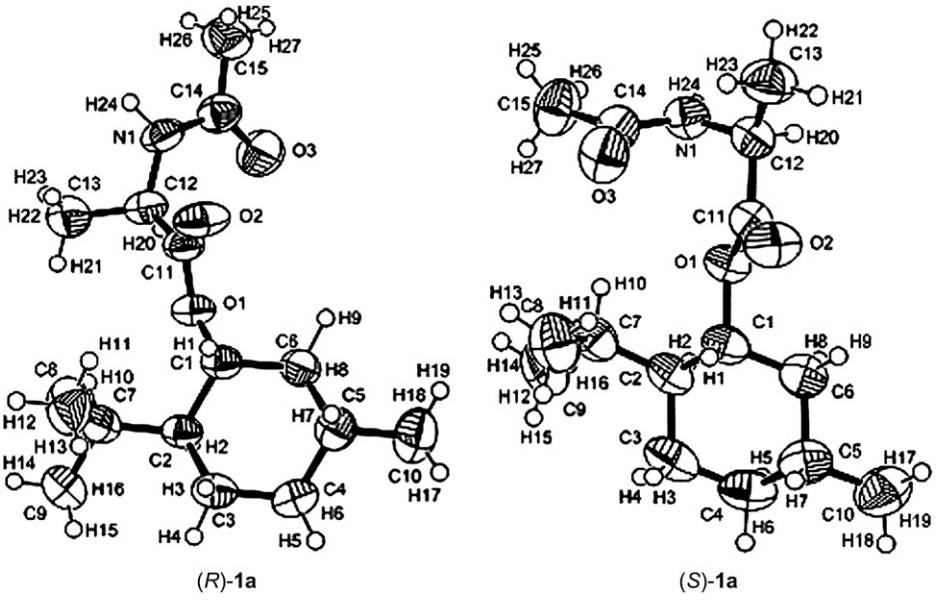

Fig. 1. ORTEP drawings of the solid-state structure of (*R*)-**1a** and (*S*)-**1a**.

Pd/C catalyst has been known to start from a coordination of olefin to the catalyst followed by the *cis*-addition of hydrogens to olefin [27].

3.2. Tin hydride reaction

Reactivity of **1** for the attack of radical species will give a clue to understand not only a stereocontrol of radical polymerization but also a stereochemistry of general organic radical reaction. Radical addition reaction of **1** with $(n\text{-}C_4H_9)_3SnH$ gave two major monoadducts with *R* and *S* configurations at newly formed chiral carbon, i.e., (*R*)-**1b** and (*S*)-**1b** (Scheme 3 and Fig. 4), in the *R*/*S* ratio of 61.9:38.1 similar to that in the hydrogenation, accompanying by other addition products and oligomers which have not yet been characterized. Good agreement of *R*/*S* ratio in hydrogenation and tin hydride reaction with s-*trans*/s-*cis* ratio of **1** indicates that the conformation of **1** regulates the configuration of the products independently on the attacking species including benzyl radical and hydrogen, and s-*trans* and s-*cis* rotamers give selectively (*R*)-**1b** and (*S*)-**1b**, respectively (Scheme 3). For the mechanism of 1,2-asymmetric induction reaction of acrylic compounds using $(n\text{-}C_4H_9)_3SnH$, characteristic allylic strain and dipole moment have been inspected, but reasonable interpretation for such a stereoselectivity has not sufficiently been achieved yet [28]. The present result obtained, i.e., asymmetric induction caused by the conformational change of the substrates may give a clue to understand a mechanism, e.g., contribution of the s-*cis* and s-*trans* conformations to the strain and dipole–dipole interaction which have already been speculated.

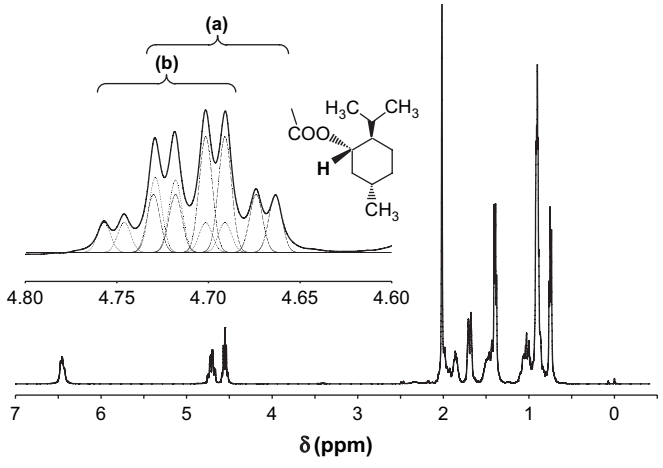

Fig. 2. ^{1}H NMR spectra of the reaction mixture produced by the hydrogenation of **1**. In expanded spectrum, (a) and (b) correspond to the absorptions due to menthyl methine proton of (*R*)-**1a** and (*S*)-**1a**, respectively.

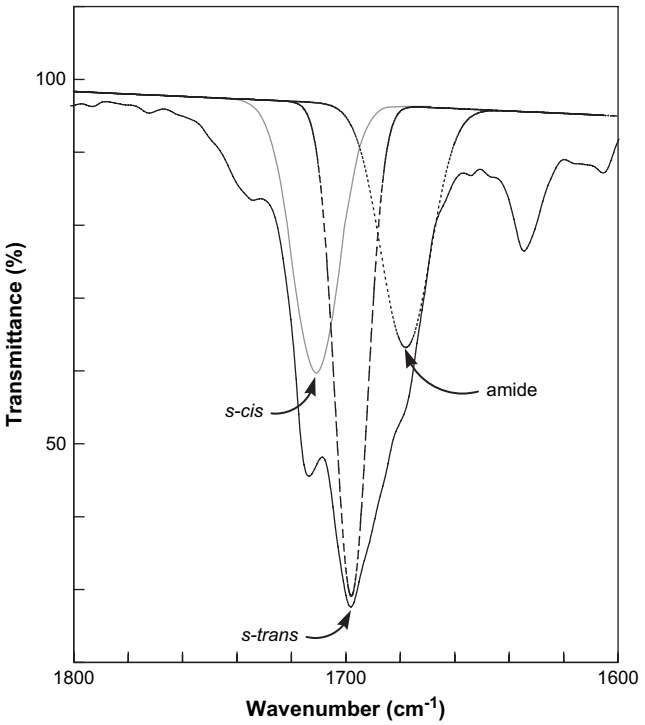

Fig. 3. IR spectrum of **1** in neat at 20 °C.

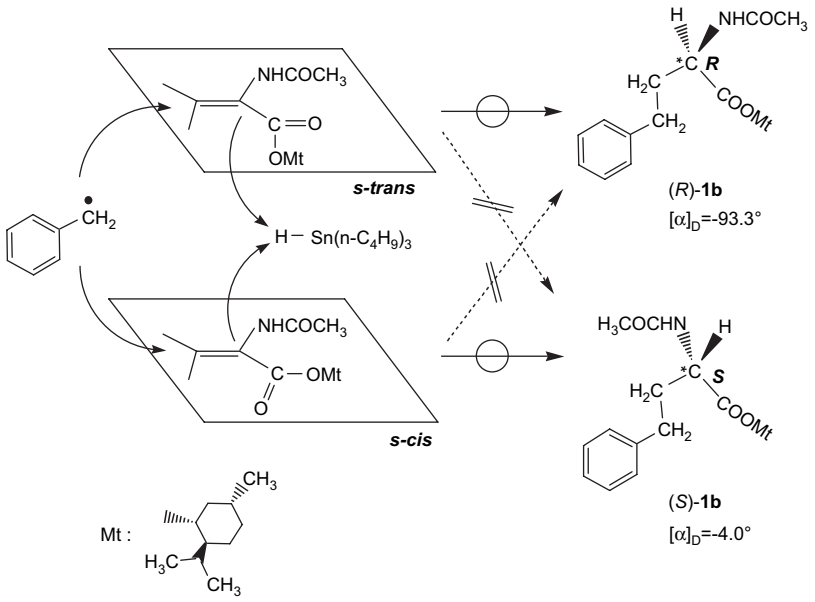

Scheme 3. Stereoselective radical addition in tin hydride reaction of **1**.

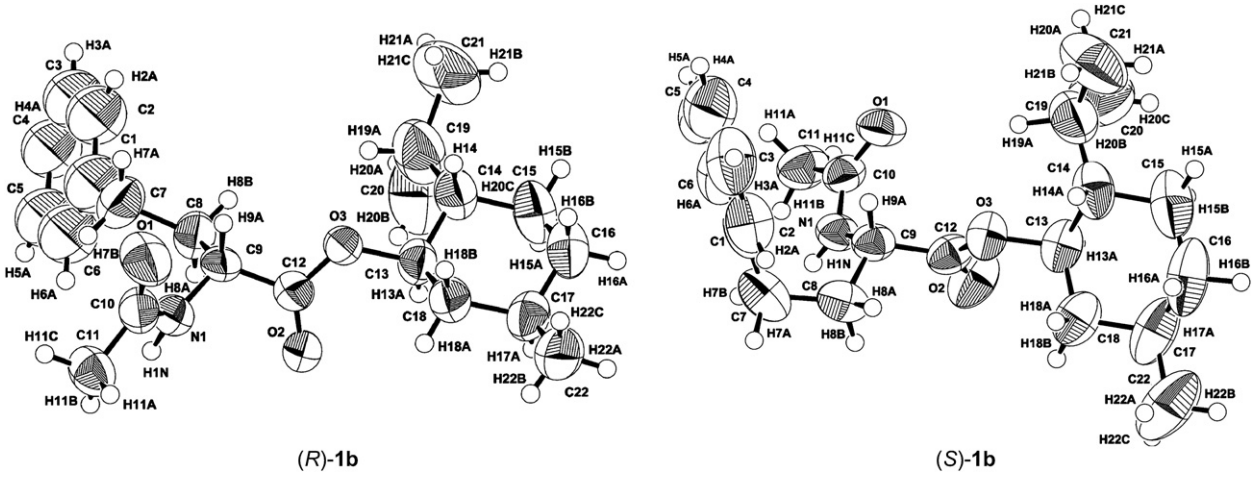

Fig. 4. ORTEP drawings of the solid-state structure of (*R*)-**1b** and (*S*)-**1b**.

3.3. Polymerization and CD spectrum

Compound **1** would easily convert to a polymer with $M_n = 3.79 \times 10^5$ and $[\alpha]_D = -96.4^\circ$ in 82.5% yield in the polymerization at 30 °C using AMVN as a radical initiator, in spite of the monomer bearing bulky substituents. Such a value of $[\alpha]_D$ for poly(**1**) is similar to that of $[\alpha]_D = -92.9^\circ$ and -93.8° obtained for random coil atactic poly((−)-menthyl methacrylate) which is prepared by the radical polymerization with benzoyl peroxide and AIBN initiators at 61 and 80 °C, respectively [29], indicating the chirality of polymer only due to a localized pendant menthyl moiety. Indeed, hydrolyzed poly(**1**) would not show any Cotton effect in the CD spectrum. In addition, poly(**1**) obtained at the temperatures much lower than T_c (75.4 °C in [**1**] = 2.0 mol/l), i.e., 6, 10 and 15 °C, in radical photopolymerization gave same CD spectrum as poly(**1**) obtained at 30 °C, suggesting that their poly(**1**)s have a similar stereostructure, and poly(**1**) obtained at 30 °C takes a random coil structure [30]. Fig. 5 represents the CD spectrum of poly(**1**) as well as that of (*R*)-**1a** and (*S*)-**1a** alone, and that of the mixture of (*R*)-**1a** and (*S*)-**1a** in 61.8:38.2 and 50:50 ratios. As clearly seen in Fig. 5, the spectrum of the polymer is in good agreement with that of (*R*)-**1a**/(*S*)-**1a** = 61.8:38.2 ratio, but obviously different from that of other ratios including 50:50 ratio.

Similar situation is also demonstrated for (*R*)-**1b** and (*S*)-**1b** which have benzyl substituent instead of hydrogen atom of **1a** as seen in Fig. 6. Basically, CD spectral pattern seems to be influenced by three-dimensional structure and stacking of chromophores, but is close to the graphical summation of individual components when chromophores are independently located in isolated domains or there is no essential interaction between chromophores at the level of secondary and tertiary structures [31] as already demonstrated in UV–vis absorption [32] and photoluminescence [33] spectroscopies where polymer composition has been determined by comparing with the spectra of each component. Little interaction between two chromophores having spatial resemblance to (*R*)-**1a** and (*S*)-**1a** forms seems to be supported by the result that the CD spectral patterns of **1a** and **1b** were similar with each other and the graphical summation of the CD spectra in the ratios of (*R*)-**1a**/(*S*)-**1a** = 61.8:38.2 ≈ (*R*)-**1b**/(*S*)-**1b** closely resembles to the spectrum of the polymer regardless of whether the substituent is hydrogen or benzyl in **1a** and **1b** [34]. Moreover, IR spectrum of poly(**1**) showed

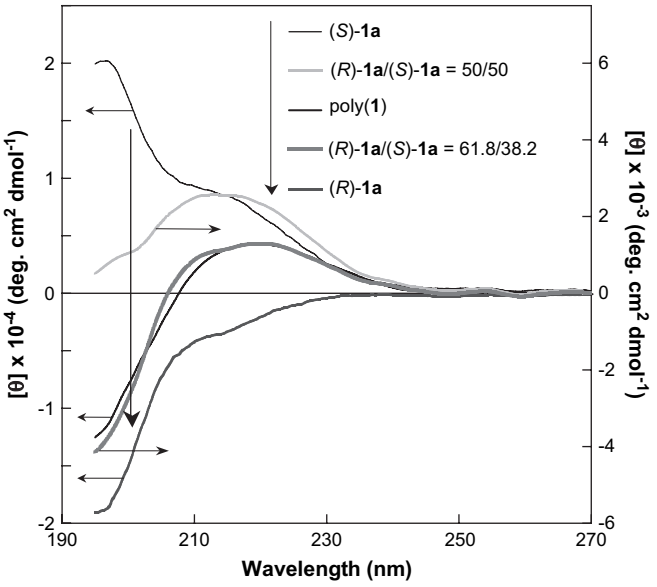

Fig. 5. CD spectra of poly(**1**), (*R*)-**1a**, (*S*)-**1a**, and mixture of (*R*)-**1a** and (*S*)-**1a** in appropriate molar ratios in *n*-hexane.

two absorptions due to a stretching of the amide carbonyl group at 1687 and 1666 cm^{-1} in ca. 62:38 ratio, which is comparable to those at 1685 and 1652 cm^{-1} for (*R*)-**1a** and (*S*)-**1a**, respectively, although more detailed study should be necessary.

3.4. ^{13}C NMR spectrum of hydrolyzed polymer

Stereochemical information of poly(**1**) was obtained from ^{13}C NMR spectrum of hydrolyzed poly(**1**), i.e., poly(potassium 2-aminoacrylate), since the hydrolyzed poly(**1**) has just one carbonyl group and represents relatively sharp ^{13}C NMR absorption in contrast to the original poly(**1**). In order to obtain a highly isotactic poly(**1**) for comparison, anionic polymerization has been carried out using *n*-C_4H_9Li as a catalyst. Unfortunately, however, no polymer was produced in such a polymerization probably due to a side reaction originated from an amide moiety in monomer since

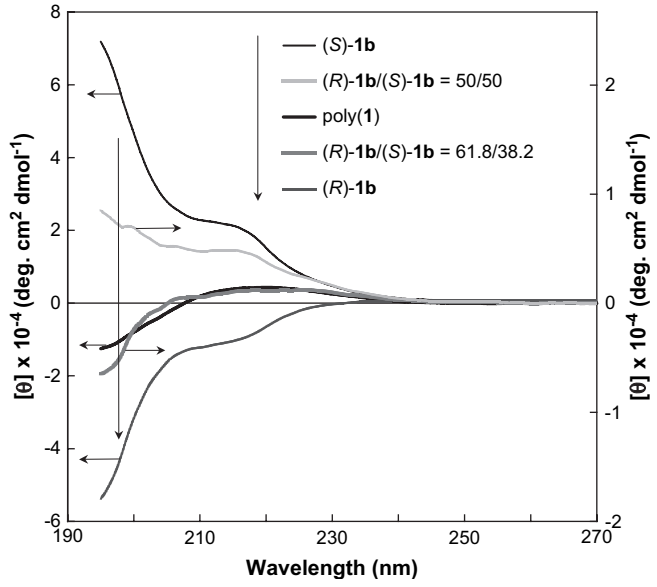

Fig. 6. CD spectra of poly(**1**), (*R*)-**1b**, (*S*)-**1b** and mixture of (*R*)-**1b** and (*S*)-**1b** in appropriate molar ratios in *n*-hexane.

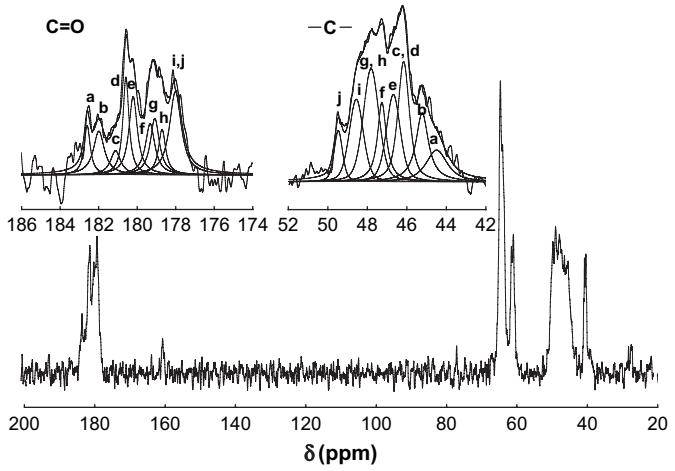

Fig. 7. ^{13}C NMR spectrum of hydrolyzed poly(**1**) and expanded spectra in the region of ester carbonyl (C═O) and main chain quaternary carbons (–C–) in D_2O at 80 °C. In expanded spectra, (a)–(j) correspond to the sequences of (a) *mrrm*, (b) *rrrm*, (c) *rrrr*, (d) *rmrm*, (e) *mmrm*, (f) *rmrr*, (g) *mmrr*, (h) *mmmm*, (i) *mmmr*, (j) *rmmr*.

2-methoxy analogy was easily polymerized to give an isotactic polymer by *n*-C_4H_9Li. As in Fig. 7, side chain carbonyl (C═O) carbon and main chain quaternary (–C–) carbon appear around 178–183 and 44–50 ppm, respectively, although noise is fairly observed in the spectrum because of a low concentration of substrate due to its low solubility and also a restricted NMR spectral accumulation due to a decomposition of internal standard dimethylsulfoxide in such a basic medium. In ^{13}C NMR spectrum of acrylate polymers, C═O [35] and –C– [36] carbons show sensitivity to the pentad stereochemistry [37]. By comparison of the NMR spectrum of hydrolyzed poly(**1**) with that of the reported acrylate polymer, the pentad sequence of hydrolyzed poly(**1**) was identified as summarized in Table 1, where *m* and *r* denote *meso* and *racemo* diads, respectively. Discrepancy in the absorption assignment and population between C═O and –C– carbon regions is small, which strongly supports the validity of the present sequence analysis.

3.5. Mechanism of polymerization

In addition to the experimental results, sequence distribution calculated from $P_R = 0.618$ and $P_S = 0.382$, probabilities that a newly formed stereogenic center in propagation will have *R* and *S* configurations by the attack of monomer, on the basis of (*R*)-**1a**/(*S*)-**1a** ratio (61.8:38.2) according to the Bovey model [38] described by Bernoullian statistics is also listed in Table 1 for comparison. In the Bovey model, for instance, *mmmm* and *rrrr* correspond to a fraction of pentad for isotactic and syndiotactic structures, respectively, and

Table 1
Assignment in terms of pentad sequences of hydrolyzed poly(**1**)

Assignment	Intensity (%)		Bernoullian
	Experimental		
	C═O	–C–	
rmmr	21.1	5.0	6.2
mmmr		12.8	13.9
mmmm	7.2	19.5	7.8
mmrr	11.2		12.4
rmrr	10.7	10.1	11.1
mmrm	14.5	13.9	13.9
rmrm	12.8	17.4	12.4
rrrr	5.4		5.0
rrrm	10.5	12.4	11.1
mrrm	6.6	8.9	6.2

they are given from the relations of $mmmm = P_m^4$ and $rrrr = P_r^4 = (1 - P_m)^4$ when P_m and P_r are defined as a probability that an attacking monomer gives the same and opposite configurations (diads *meso* and *racemo*, respectively) as that of the last unit at its proceeding unit, in which P_m and P_r are expressed as $P_m = P_R^2 + P_S^2$ and $P_r = 2P_RP_S$. So far P_R and P_S have been obtained as a relative value from the diad or triad *meso* and *racemo* ratios determined by NMR. Thus, the independent evaluation of P_R and P_S from the molar ratio of hydrogenation products or CD spectral analysis should provide more precise structural and mechanistic informations. As seen in Table 1, the sequence distribution of hydrolyzed poly(**1**) is comparable to that predicted by the Bernoullian statistics.

In contrast to the Bovey sequence where the stereochemistry in propagation is influenced only by the stereochemistry of the ultimate unit (ultimate unit effect), the first-order Markov sequence [39] is generated by the propagating steps in which the direction of monomer addition is influenced by the stereochemistry of the penultimate unit (penultimate unit effect). For the verification of such a penultimate unit effect, a quantity of $4(mm)(rr)/(mr)^2$ has often been employed [40], and it becomes unity in the polymerization proceeded according to the Bovey model. Large deviation of $4(mm)(rr)/(mr)^2$ value from unity is then used as a measure of penultimate unit effect character. For chain-end controlled polymerization (ultimate unit effect), for instance, such a value has specifically taken 1.07, 0.97, and 0.94 for the polymerizations of MMA [41], methyl 2-phenylacrylate [42], and (−)-menthyl methacrylate [43], respectively [44], whereas in the polymerization allowing the penultimate unit effect, that value fairly deviates from unity, e.g., 2.40–6.95 [45] and 0.32–0.47 [46]. The value of 1.05 obtained in the present study is close to that of the chain-end controlled polymerization, and it is much lower than that of the sterically-hindered radical polymerization of triphenylmethyl methacrylate (5.33) [47] and isospecific chiral auxiliary radical polymerization of oxazolidine acrylamides (92.0) [16]. Although it is not possible, from the quantity of $4(mm)(rr)/(mr)^2$ and pentad sequence alone, to obtain a complete description of the polymerization mode of **1** without additional informations on the polymerization, e.g., NMR analysis of polymer sequence at higher level and thermodynamic analysis of $4(mm)(rr)/(mr)^2$ value [40], polymerization of **1** would proceed through the Bovey model.

Although the fit of the experimental data to a simple model provides support for but does not prove that model, the results obtained in this study seem to suggest that the stereocontrol in the

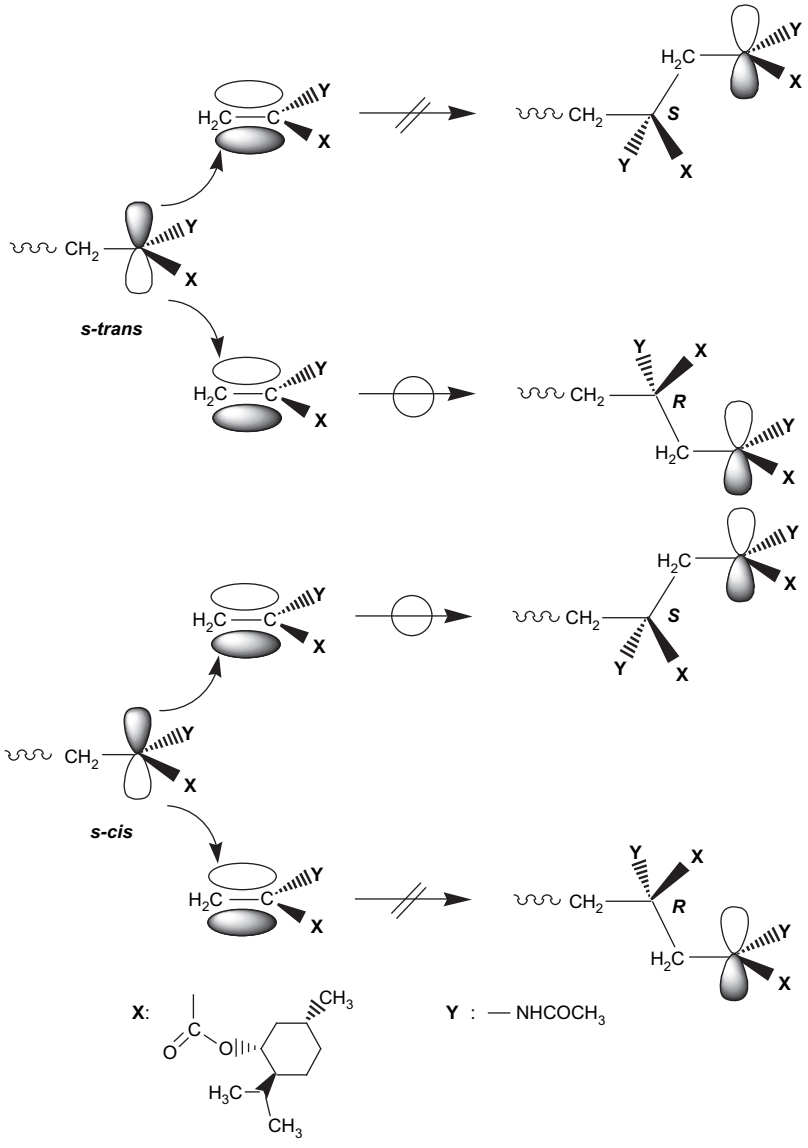

Scheme 4. Stereoselective propagation in radical polymerization of **1**.

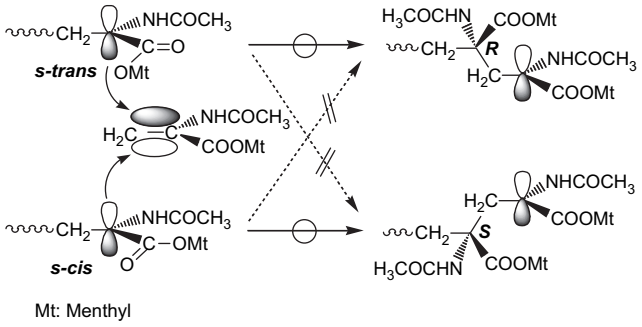

Scheme 5. Conformation-controlled radical polymerization of **1**.

polymerization of **1** arises from a facial selectivity due to the s-*trans* and s-*cis* conformations of the growing polymer radical end in monomer addition [48]. Such a selectivity may be supposed to be induced by a steric hindrance in an approach of monomer to the front or back face of the radical depending on the s-*cis* or s-*trans* conformation of the radical, in which the growing polymer radical presumably takes the s-*cis* and s-*trans* conformations similar to monomer since the growing chain end and olefinic carbons take a similar conjugated planar sp^2 configuration with each other [49] and actually the radical reaction of **1** using tin hydride would proceed with high stereoselectivity as the same manner as the polymerization. Thus, as in Scheme 4, most of the s-*trans* and s-*cis* conformers of the growing polymer radical will selectively add to the monomer to give *S* and *R* configurations, respectively, at newly formed chiral quaternary carbon. Such a controlled polymerization, so-called conformation-controlled radical polymerization, continues throughout the polymerization, and for instance an isotactic sequence can be generated from a continuous selective propagation of same conformational monomers, e.g., *cis*–*cis*–*cis* (*S*–*S*–*S*) and *trans*–*trans*–*trans* (*R*–*R*–*R*) sequences. During a propagation, rotation around the terminal main chain C–C bond of the growing polymer radical is of course possible, but even in such a case the propagation will mostly proceed stereospecifically without configurational inversion. The agreement between the s-*trans*/s-*cis* monomer ratio and the spatial *R*/*S* structural ratio of polymer suggests that the polymerization reactivity of s-*trans* and s-*cis* conformers of **1** resembles with each other, and it excludes a penultimate effect in tacticity in the present polymerization conditions.

Tacticity, however, is not always controlled by a monomer conformation [50]. A number of 1,2-unsaturated carbonyl compounds including acrylates and vinyl ketones, for instance, takes 100% s-*trans* conformation at normal temperature and in normal atmospheric pressure [51], but they have produced an atactic polymer in normal radical polymerization [46,52]. It is considered that the stereochemistry in radical polymerization is dominated by the reaction profiles including kinetic and thermodynamic controls, rates of propagation and interconversion of monomer conformation, selectivity of radical for the attack of monomer, hydrogen-bonding, salvation, and so forth. In the case of **1**, the rate of *trans*–*cis* isomerization will compete with the propagation rate, and the rotation around C(=C)–C(=O) bond of **1** may be relatively slow compared with a propagation rate because of the bulky substituents and a facile propagation due to the captodative substitution [53].

4. Conclusion

We have been interested in the subject how tacticity can arise in free radical polymerization of acrylates, which has been in chaos for a long time. We have believed that there should be some rule regarding to a tacticity even in an atactic polymerization. In the present study, it was demonstrated that the growing polymer radical end could control a stereochemistry of free radical polymerization as shown in Scheme 5 depending on the s-*trans* and s-*cis* conformations. The results obtained here will give a clue to understand some unresolved problems including a stereoselective polymerization controlled by additives [4–6,9,10] and also to design the stereospecific polymers including isospecific and helical polymers through a radical mechanism.

Acknowledgment

We thank Prof. Y. Miura at Osaka City University for the measurement of X-ray diffraction.

Appendix. Supplementary data

The CIF files contain X-ray structure data of (*R*)-**1a**, (*S*)-**1a**, (*R*)-**1b**, and (*S*)-**1b**. Supplementary data associated with this article can be found in the online version, at doi:10.1016/j.polymer.2008.06.042.

References

[1] (a) Nakano T, Okamoto Y. Chem Rev 2001;101:4013–38;
(b) Sibi MP, Manyem S, Zimmerman J. Chem Rev 2003;103:3263–95.
[2] (a) Luts J-F, Neugebauer D, Matyjaszewski K. J Am Chem Soc 2003;125:6986–93;
(b) Luts J-F, Jakubowski W, Matyjaszewski K. Rapid Commun 2004;25:486–92;
(c) Yu Miura, Shibata T, Satoh K, Kamigaito M, Okamoto Y. J Am Chem Soc 2006;128:16026–7.
[3] Tanaka H. Prog Polym Sci 1992;17:1107–52.
[4] Baraki H, Habaue S, Okamoto Y. Macromolecules 2001;34:4724–9.
[5] Mero CL, Porter N. J Org Chem 2000;65:775–81.
[6] Buter R, Tan YY, Challa G. J Polym Sci Polym Chem Ed 1973;11:2975–89.
[7] (a) Tanaka H, Sakai I, Ota T. J Am Chem Soc 1986;108:2208–11;
(b) Tanaka H, Yasuda Y, Ota T. Chem Commun 1986:109–10;
(c) Tanaka H, Sasai K, Sato T, Ota T. Macromolecules 1988;21:3534–6.
[8] Okamoto Y, Habaue S, Isobe Y, Saito Y. Macromol Symp 2003;195:75–80.
[9] Buter R, Tan YY, Challa G. J Polym Sci Polym Chem Ed 1973;11:989–97.
[10] Buter R, Tan YY, Challa G. J Polym Sci Polym Chem Ed 1972;10:1031–49.
[11] Yuki H, Hatada K, Niinomi T, Kikuchi Y. Polym J 1970;1:36–45.
[12] Hoshikawa N, Hotta Y, Okamoto Y. J Am Chem Soc 2003;125:12380–1.
[13] Okamoto Y, Habaue S, Isobe Y, Nakano T. Macromol Symp 2002;194:83–8.
[14] Porter NA, Swann E, Nally J, McPhail AT. J Am Chem Soc 1990;112:6740–1.
[15] Porter NA, Breyer RA, Swann E, Nally J, Predhan J, Allen T, et al. J Am Chem Soc 1991;113:7002–10.
[16] Porter NA, Allen TR, Breyer RA. J Am Chem Soc 1992;114:7676–83.
[17] Curran DP, Shen W, Zhang J, Heffner TA. J Am Chem Soc 1990;112:6738–40.
[18] Giese B, Zehnder M, Roth M, Zeitz H-G. J Am Chem Soc 1990;112:6741–942.
[19] Ashraf SA, Kane-Maguire LAP, Pyne SG, Wallace G. Macromolecules 1998;31:8737–43.
[20] Moad G, Solomon DH. The chemistry of free radical polymerization. Oxford UK: Pergamon Press; 1995.
[21] Monomer is consumed along with a progress of polymerization, and in the final stage of the polymerization monomer concentration becomes very low. Consequently a polymerization temperature gradually comes close to T_c since T_c is known to be proportional to the reciprocal of monomer concentration as given by $1/T_c = (R/\Delta G^o)\ln[\text{monomer}]_e$, where R, ΔG^o, and $[\text{monomer}]_e$ denote gas constant, standard free energy, and monomer concentration in equilibrium, respectively. In such a condition, it is possible to change drastically the polymer structures including tacticity. Thus, the polymerization of **1** which

has relatively low T_c easily approaches T_c along with a progress of polymerization even in a conventional condition, which results in the exceptional chiroptical phenomena including change of specific rotation of polymer and helix formation due to an isospecific polymerization.
See Ref.: Tanaka H, Niwa H. Proceedings of 227th ACS National Meeting, vol. 45; 2004. p. 1047–8.
Tanaka H, Niwa H. Proceedings of 40th International Symposium on Macromolecules; 2004. P2.1-140.
Niwa M, Tanaka H. Polym Prepr Jpn 2007;56:3290.
[22] Tanaka H, Niwa M. Polymer 2005;46:4635–9.
[23] Royles BJL, Sherrington DC. Chem Commun 1998:421–2.
[24] Altomare A, Cascarano M, Giacovazzo C, Guagliardi A. J Appl Crystallogr 1993; 26:343–50.
[25] Sheldrick GM. SHELX97: program for crystal structure solution. Göttingen Germany: University of Göttingen; 1997.
[26] (a) Takekiyo T, Kato M, Taniguchi Y. J Mol Liq 2005;119:147–52;
(b) Yamashita T, Ishii K, Hasegawa M. J Photochem Sci Technol 2007;20:763–6.
[27] Jenkins JW. Platinum Met Rev 1984;28:98–106.
[28] Porter NA, Bruhnke JD, Wu W-X, Rosenstein IJ, Breyer RA. J Am Chem Soc 1991;113:7788–90.
[29] Sobue H, Matsuzaki K, Nakano S. J Polym Sci Part A Polym Chem 1964;2:3339–46.
[30] In the polymerization at the temperature much lower than T_c (75.4 °C), e.g., near 10 °C, **1** has been reported to give a random coil polymer.
See Ref.: Tanaka H, Niwa M Polymer 2007;48:3999–4000. and Ref. [22].
[31] Pasto DJ, Johnson CR. Organic structure determination. Englewood Cliffs NJ: Prentice-Hall Inc; 1969.
[32] (a) Garcia-Rubio LH. J Appl Polym Sci 1982;27:2043–52;
(b) Asami R, Takaki M, Matsuse T. Makromol Chem 1989;190:45–51.
[33] (a) Duhamel J, Khaykin Y, Hu YZ, Winnik MA, Boileau S, Mechin F. Eur Polym J 1994;30:129–34;
(b) Fakayode SO, Williams AA, Busch MA, Busch KW, Warner IJ. Fluorescence 2006;16:659–70.
[34] The correlation of $R/S \approx 62{:}38$ in the CD spectrum of the polymer would not indicate the chiroptical contents of *R* and *S* configurations of 62 and 38%. Symbol of "*R*" for a quaternary carbon on the polymer backbone, for instance, does not represent a real chiroptical *R*, but a spatial resemblance to *R* form of the model compound.
[35] Solaro R, Altomare A. Polym J 1990;22:497–501.
[36] Pathak CP, Patni MC, Babu GN. Macromolecules 1986;19:1035–42.
[37] Hatada K, Kitayama T, Ute K. Prog Polym Sci 1988;13:189–276.
[38] (a) Bovey FA. High resolution NMR of macromolecules. New York: Academic Press; 1972;
(b) Bovey FA. Chain structure and conformation of macromolecules. New York: Academic Press; 1982.
[39] (a) Merz E, Alfrey T, Goldfinger G. J Polym Sci 1946;1:75–82;
(b) Ham GE. J Polym Sci 1954;14:87–93.
[40] Chujo R. J Phys Soc Jpn 1966;21:2669–73.
[41] Bovey FA, Tiers GVD. J Polym Sci 1960;44:173–82.
[42] Yuki H, Hatada K, Niinomi T, Hashimoto M, Ohshima J. Polym J 1971;2: 629–39.
[43] Nakano T, Mori M, Okamoto Y. Macromolecules 1993;26:867–9.
[44] The quantity of $4(mm)(rr)/(mr)^2$ corresponds to the rate ratio of $(k_{mm}/k_{mr})/(k_{rm}/k_{rr})$, where k_{mm}, for instance, denotes a rate constant of *meso*-propagation of the polymer radical having terminal *meso* unit. Thus the equation of $4(mm)(rr)/(mr)^2 = 1$ does not always exclude a penultimate unit effect.
[45] Buter R, Tan YY, Challa G. J Polym Sci Polym Chem Ed 1973;11:1013–24.
[46] Hirano T, Yamada B. Polymer 2003;44:4481–6.
[47] Nakano T, Matsuda A, Okamoto Y. Polym J 1996;28:556–8.
[48] Tacticity control of **1** by conformation seems to be performed not only by the s-*cis* and s-*trans* isomerizations but also by the chiral substituents including menthyl moiety since (+)-menthyl analogy gives a opposite sense helical polymer in the polymerization near ceiling temperature. See Ref. [22].
[49] Most of the propagating radical have been known to take a nearly planar sp^2 structure although it has been reported on the basis of the molecular orbital calculation for 1,1-disubstituted conjugated olefins that a propagating radical does not always take a conjugated planar structure as seen in monomer in the transition state.
See Ref.: Huang DM, Monteire MJ, Gilbert RG Macromolecules 1998;31: 5175–87.
[50] Seeman JI. Chem Rev 1983;83:83–134.
[51] (a) Faulk DD, Fry A. J Org Chem 1983;35:364–9;
(b) Abraham RJ, Mobli M, Ratti J, Sancassan F, Smith TMD. J Phys Org Chem 2006;19:384–92.
[52] Ivin KJ. Annu Rep Prog Chem Sect A 1970;66:121–49.
[53] Tanaka H. Prog Polym Sci 2003;28:1171–203.